TECHNISCHE UNIVERSITÄT
KAISERSLAUTERN

A Second Order Non-smooth Variational Model for Restoring Manifold-valued Images

Ronny Bergmann*

Mathematical Image Processing and Data Analysis
Department of Mathematics
University of Kaiserslautern

July 10, 2015

25th Rhein-Main Arbeitskreis – Mathematics of Computation, Darmstadt

FELIX KLEIN
ZENTRUM FÜR
MATHEMATIK

*joint work with M. Bačák (Télécom ParisTech), G. Steidl (U Kaiserslautern), A. Weinmann (TU Munich)

Contents

Restoring Images: Denoising and Inpainting

- given noisy image $f\colon \mathcal{V} \to \mathbb{R}$, $\mathcal{V} \subseteq \mathcal{G} = \{1,\ldots,N\} \times \{1,\ldots,M\}$
- reconstruct original image $u_0\colon \mathcal{G} \to \mathbb{R}$
- pixel from $\mathcal{G}\backslash\mathcal{V}$ have to be inpainted
- approach: Minimize variational model

$$\mathcal{E}(u) := \underbrace{F(f,u)}_{\text{data term}} + \underbrace{\alpha\, R(u)}_{\text{regularization term}}, \qquad \alpha > 0$$

- first order models (total variation, TV)
  - isotropic model with discrete gradient $|\nabla u|$:

$$R_{\text{iso}}(u) := \sum_{i,j} |\nabla u| = \sum_{i,j} \sqrt{|u_{i+1,j} - u_{i,j}|^2 + |u_{i,j+1} - u_{i,j}|^2}$$

  - anisotropic model:

$$R_{\text{aniso}}(u) := \sum_{i,j} \bigl(|u_{i+1,j} - u_{i,j}| + |u_{i,j+1} - u_{i,j}|\bigr)$$

Denoising Gray-valued Images

A drawback of first order models

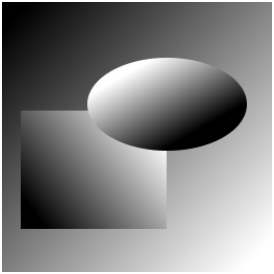
original

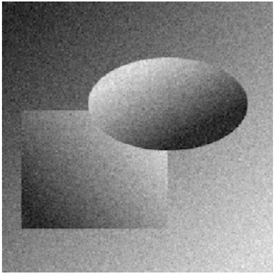
noisy

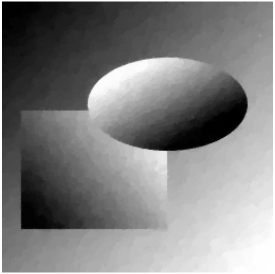
first order model

Denoising Gray-valued Images

A drawback of first order models and a remedy.

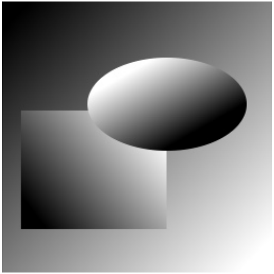
original

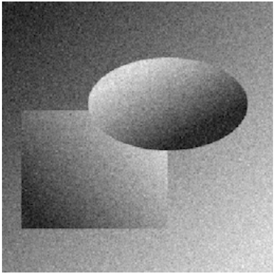
noisy

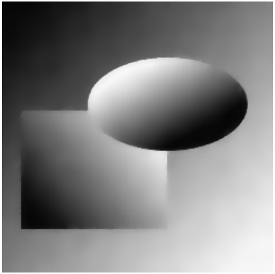
second order model

Riemannian Manifolds

Here: Images with pixel values in a Riemannian manifold $\mathcal{M}$

Goal: Second Order Model for images $f\colon \mathcal{V} \to \mathcal{M}$

Applications with manifold-valued images

$\mathbb{S}^1$ InSAR, HSI(HSV) color space, phase space

$\mathbb{S}^2$ directions, chromaticity-brightness colorspace

$\mathrm{SO}(3)$ orientations, electron backscattered diffraction

$\mathcal{P}(s)$ DT-MRI, covariance matrices

Symmetric Positive Definite Matrices: $x^{\mathrm{T}}Ax > 0$.

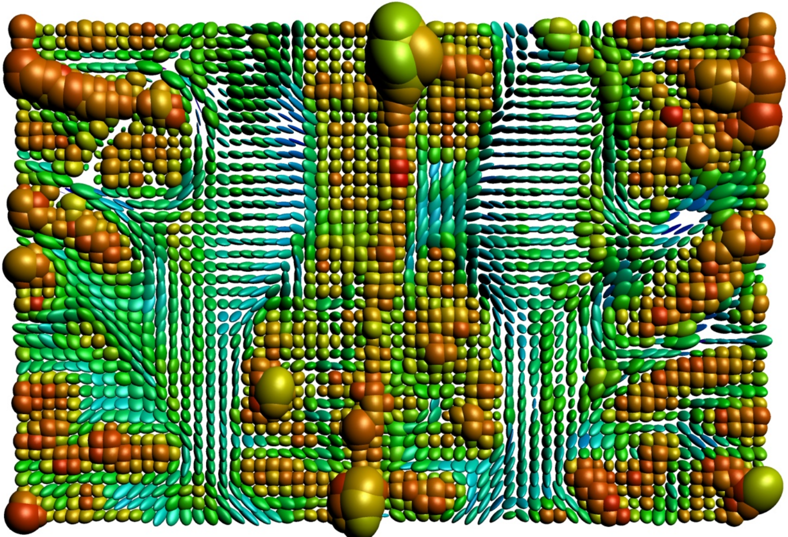

each pixel is a 3×3 symmetric positive definite matrix, ellipsoids: $x^{\mathrm{T}}Ax = 1$

First and Second Order Differences

Let's restrict ourselves to signals for now... $\mathcal{G} = \{1, \ldots, N\}, \mathcal{V} \subset \mathcal{G}$

On $\mathbb{R}^n$

- line $\gamma(t) = x + t(y - x)$
- distance $\|x - y\|_2$
- first order model

$$\sum_{i \in \mathcal{V}} \|f_i - u_i\|_2^2 + \alpha \sum_{i \in \mathcal{G} \setminus \{N\}} \|u_i - u_{i+1}\|_2$$

Riemannian manifold $\mathcal{M}$

- geodesic path $\gamma_{\overset{\frown}{x,z}}(t)$
- geodesic distance $d\colon \mathcal{M} \times \mathcal{M} \to \mathbb{R}_{\geq 0}$
- first order model

$$\sum_{i \in \mathcal{V}} d(f_i, u_i)^2 + \alpha \sum_{i \in \mathcal{G} \setminus \{N\}} d(u_i, u_{i+1})$$

First and Second Order Differences

Let's restrict ourselves to signals for now...

$\mathcal{G} = \{1, \ldots, N\}, \mathcal{V} \subset \mathcal{G}$

On $\mathbb{R}^n$

- line $\gamma(t) = x + t(y - x)$
- distance $\|x - y\|_2$
- first order model

$$\sum_{i\in\mathcal{V}} \|f_i - u_i\|_2^2 + \alpha \sum_{i\in\mathcal{G}\setminus\{N\}} \|u_i - u_{i+1}\|_2$$

- second oder difference

$$\|x - 2y + z\|_2$$

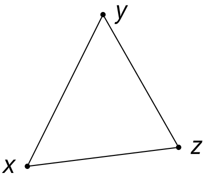

Riemannian manifold $\mathcal{M}$

- geodesic path $\gamma_{\overset{\frown}{x,z}}(t)$
- geodesic distance $d\colon \mathcal{M} \times \mathcal{M} \to \mathbb{R}_{\geq 0}$
- first order model

$$\sum_{i\in\mathcal{V}} d(f_i, u_i)^2 + \alpha \sum_{i\in\mathcal{G}\setminus\{N\}} d(u_i, u_{i+1})$$

- How to model that on $\mathcal{M}$?

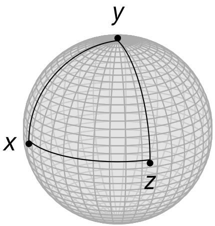

First and Second Order Differences

Let's restrict ourselves to signals for now... $\mathcal{G} = \{1, \ldots, N\}, \mathcal{V} \subset \mathcal{G}$

On $\mathbb{R}^n$

- line $\gamma(t) = x + t(y - x)$
- distance $\|x - y\|_2$
- first order model

$$\sum_{i \in \mathcal{V}} \|f_i - u_i\|_2^2 + \alpha \sum_{i \in \mathcal{G} \setminus \{N\}} \|u_i - u_{i+1}\|_2$$

- second oder difference

$$2\|\tfrac{1}{2}(x + z) - y\|_2$$

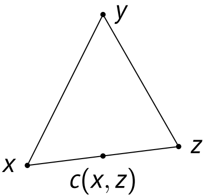

Riemannian manifold $\mathcal{M}$

- geodesic path $\gamma_{\widehat{x,z}}(t)$
- geodesic distance $d\colon \mathcal{M} \times \mathcal{M} \to \mathbb{R}_{\geq 0}$
- first order model

$$\sum_{i \in \mathcal{V}} d(f_i, u_i)^2 + \alpha \sum_{i \in \mathcal{G} \setminus \{N\}} d(u_i, u_{i+1})$$

- idea: mid point formulation

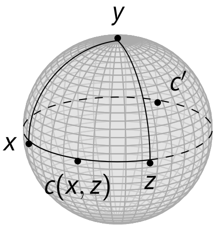

First and Second Order Differences

Let's restrict ourselves to signals for now... $\mathcal{G} = \{1, \ldots, N\}, \mathcal{V} \subset \mathcal{G}$

On $\mathbb{R}^n$

- line $\gamma(t) = x + t(y - x)$
- distance $\|x - y\|_2$
- first order model

$$\sum_{i\in\mathcal{V}} \|f_i - u_i\|_2^2 + \alpha \sum_{i\in\mathcal{G}\setminus\{N\}} \|u_i - u_{i+1}\|_2$$

- second oder difference

$$2\|c(x,z) - y\|_2, \quad c(x,y)\colon \text{ mid point}$$

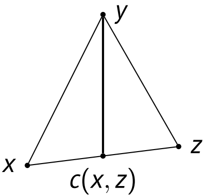

Riemannian manifold $\mathcal{M}$

- geodesic path $\gamma_{\widehat{x,z}}(t)$
- geodesic distance $d\colon \mathcal{M} \times \mathcal{M} \to \mathbb{R}_{\geq 0}$
- first order model

$$\sum_{i\in\mathcal{V}} d(f_i, u_i)^2 + \alpha \sum_{i\in\mathcal{G}\setminus\{N\}} d(u_i, u_{i+1})$$

- idea: mid point formulation

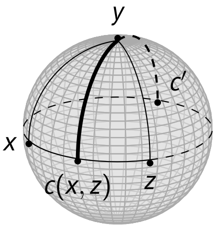

A Second Order TV-type Model

Mid points between $x, z \in \mathcal{M}$:

$$\mathcal{C}_{x,z} := \left\{c \in \mathcal{M} : c = \gamma_{\overset{\frown}{x,z}}\left(\tfrac{T}{2}\right) \text{ for any geodesic } \gamma_{\overset{\frown}{x,z}},\quad T := \mathcal{L}(\gamma_{\overset{\frown}{x,z}})\right\}$$

The Absolute Second Order Difference:

$$d_2(x,y,z) := \min_{c \in \mathcal{C}_{x,z}} d(c,y), \qquad x,y,z \in \mathcal{M}.$$

$\Rightarrow$ Second Order TV-type Model for $\mathcal{M}$-valued signals f

$$\mathcal{E}(u) := \sum_{i\in\mathcal{V}} d(f_i,u_i)^2 + \alpha \sum_{i\in\mathcal{G}\setminus\{N\}} d(u_i,u_{i+1}) + \beta \sum_{i\in\mathcal{G}\setminus\{1,N\}} d_2(u_{i-1},u_i,u_{i+1})$$

Example: The Circle $\mathbb{S}^1$

Cyclic data: $p, q, r \in \mathbb{S}^1 := \{s \in \mathbb{R}^2 \ : \ \|s\|_2 = 1\} \Longleftrightarrow x, y, z \in [-\pi, \pi)$

$d_2(x, y, z)$: Several unwrappings

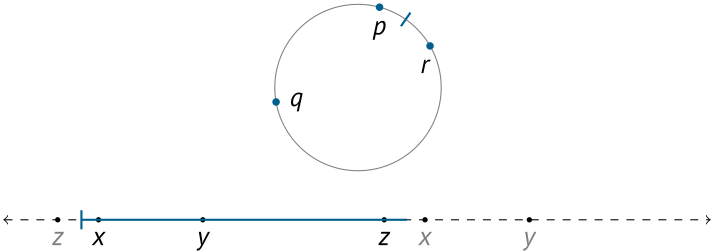

$$|x - 2y + z|$$

Example: The Circle $\mathbb{S}^1$

Cyclic data: $p, q, r \in \mathbb{S}^1 := \{s \in \mathbb{R}^2 : \|s\|_2 = 1\} \Longleftrightarrow x, y, z \in [-\pi, \pi)$

$d_2(x,y,z)$: Several unwrappings

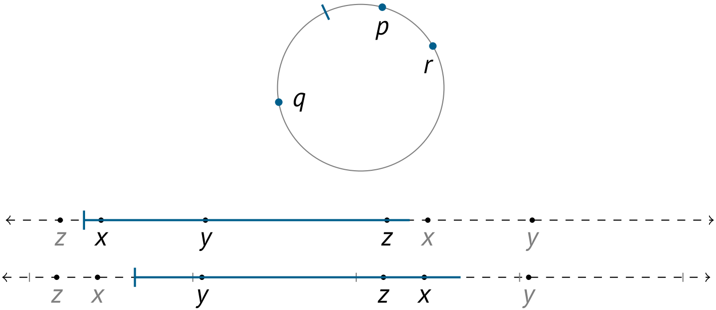

$$|x - 2y + z|$$

Example: The Circle $\mathbb{S}^1$

Cyclic data: $p, q, r \in \mathbb{S}^1 := \{s \in \mathbb{R}^2 \ : \ \|s\|_2 = 1\} \Longleftrightarrow x, y, z \in [-\pi, \pi)$

$d_2(x, y, z)$: Several unwrappings

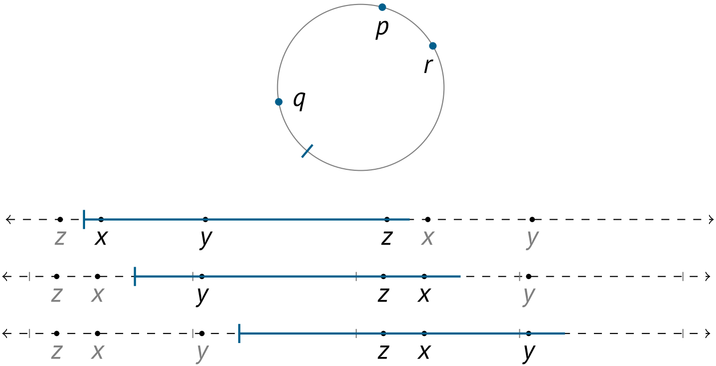

$$|x - 2y + z|$$

Example: The Circle $\mathbb{S}^1$

Cyclic data: $p, q, r \in \mathbb{S}^1 := \{s \in \mathbb{R}^2 : \|s\|_2 = 1\} \Longleftrightarrow x, y, z \in [-\pi, \pi)$

$d_2(x, y, z)$: Minimize over all unwrappings

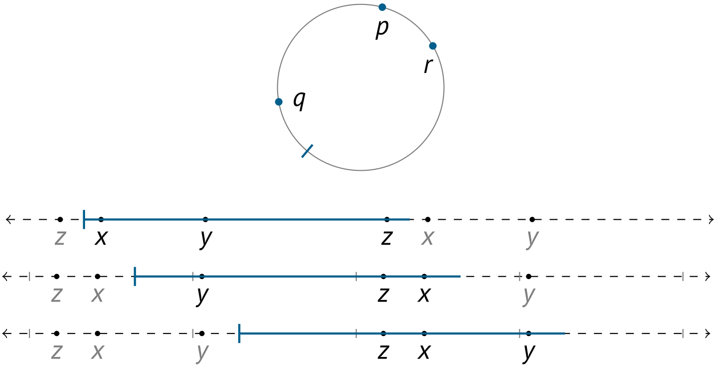

$$d_2(x, y, z) := \min_{\mu \in \mathbb{R}} \big|(x + \mu) - 2(y + \mu) + (z + \mu)\big| = |(x - 2y + z)_{2\pi}|$$

Proximal Mappings

Proximal algorithms are standard tool for solving non-smooth, constrained minimization problems.

To compute a minimizer of $\mathcal{E}(u)$ we need proximal mappings

For a proper, closed, convex function $\varphi\colon \mathbb{R}^n \to (-\infty, +\infty]$ and $\lambda > 0$ the proximal mapping is defined by [Moreau, 1965; Rockafellar, 1976]

$$\operatorname{prox}_{\lambda\varphi}(g) := \operatorname*{arg\,min}_{u\in\mathbb{R}^n} \frac{1}{2}\|u-g\|_2^2 + \lambda\varphi(u).$$

For a function $\varphi\colon \mathcal{M}^n \to (-\infty, +\infty]$ and $\lambda > 0$ the proximal mapping is defined by [Ferreira, Oliveira, 2002]

$$\operatorname{prox}_{\lambda\varphi}(g) := \operatorname*{arg\,min}_{u\in\mathcal{M}^n} \frac{1}{2}\sum_{i=1}^{n} d(u_i, g_i)^2 + \lambda\varphi(u).$$

Note: For a minimizer u^* of φ it holds $\operatorname{prox}_{\lambda\varphi}(u^*) = u^*$.

The Cyclic Proximal Point Algorithm

To find $\arg\min_x \varphi(x)$ use Picard iteration: Proximal Point Algorithm

$$x^{(k)} = \operatorname{prox}_{\lambda\varphi}(x^{(k-1)}), \quad k > 0$$

$\Rightarrow$ fast evaluation of $\operatorname{prox}_{\lambda\varphi}$ needed

For $\varphi = \sum_{l=1}^{c} \varphi_l$ use Cyclic Proximal Point Algorithm (CPPA) [Bertsekas, 2011]

$$x^{(k+\frac{l+1}{c})} = \operatorname{prox}_{\lambda_k\varphi_l}(x^{(k+\frac{l}{c})}), \quad i = 0, \ldots, c-1,\ k > 0$$

For real-valued data:
Converges to a minimizer if $\{\lambda_k\} \in \ell_2(\mathbb{Z})\setminus\ell_1(\mathbb{Z})$.

Minimizing the Second Order Model

To minimize

$$\mathcal{E}(u) := \sum_{i\in\mathcal{V}} d(f_i,u_i)^2 + \alpha \sum_{i\in\mathcal{G}\setminus\{N\}} d(u_i,u_{i+1}) + \beta \sum_{i\in\mathcal{G}\setminus\{1,N\}} d_2(u_{i-1},u_i,u_{i+1})$$

take each summand as one φ_l in the CPPA.
For the involved proximal maps we have

- $\varphi(u_i) = d(f_i,u_i)^2$, analytical solution [Ferreira, Oliveira, 2002]
- $\varphi(u_i,u_{i+1}) = d(u_i,u_{i+1})$, analytical solution [Weinmann, Storath, Demaret, 2014]
- $\varphi(u_{i-1},u_i,u_{i+1}) = d_2(u_{i-1},u_i,u_{i+1})$
  - analytical solution for $\mathbb{S}^1$ [B., Laus, Steidl, Weinmann, 2014]
  - numerical solution otherwise [Bačák, B., Steidl, Weinmann, 2015]

A Proximal Mapping on $\mathbb{S}^1$

Theorem [B., Laus, Steidl, Weinmann, 2014]

The minimizer(s) of

$$\operatorname{prox}_{\lambda d_2}(g) = \operatorname*{arg\,min}_{u \in (\mathbb{S}^1)^3} \Bigl\{ \frac{1}{2} \sum_{j=1}^{3} d(u_j, g_j)^2 + \lambda d_2(u_1, u_2, u_3) \Bigr\}$$

are given using

$$s := \operatorname{sgn}(g_1 - 2g_2 + g_3)_{2\pi},\ w := (1, -2, 1)^{\mathrm{T}},\ \text{and } m := \min\Bigl\{\lambda, \frac{1}{6}|(\langle g, w\rangle)_{2\pi}|\Bigr\}$$

as

1. if $|(\langle g, w\rangle)_{2\pi}| < \pi$ by $\operatorname{prox}_{\lambda d_2}(g) = (g - smw)_{2\pi}$
2. if $|(\langle g, w\rangle)_{2\pi}| = \pi$ by $\operatorname{prox}_{\lambda d_2}(g) = (g \pm smw)_{2\pi}$

Proximal Mapping of a Second Order Difference on $\mathcal{M}$

To Compute

$$\operatorname{prox}_{\lambda d_2}(g) = \operatorname*{arg\,min}_{u\in\mathcal{M}^3}\Big\{\frac{1}{2}\sum_{i=1}^{3} d(u_i,g_i)^2 + \lambda d_2(u_1,u_2,u_3)\Big\}$$

(sub)gradient descent method requires gradient of $d_2(x,y,z) = d(c(x,z),y)$

$$\nabla_{\mathcal{M}^3} d_2 = \left(\nabla_{\mathcal{M}} d_2(\cdot,y,z), \nabla_{\mathcal{M}} d_2(x,\cdot,z), \nabla_{\mathcal{M}} d_2(x,y,\cdot)\right)^{\mathrm{T}}.$$

For $y \neq c(x,z)$ and an ONB $\{\xi_1,\ldots,\xi_n\}$ of $T_x\mathcal{M}$

- $\nabla_{\mathcal{M}} d_2(x,\cdot,z)(y) = \dfrac{\log_y c(x,z)}{\|\log_y c(x,z)\|_y} \in T_y\mathcal{M}$
- $\nabla_{\mathcal{M}} d_2(\cdot,y,z)$ by chain rule

$$\nabla_{\mathcal{M}} d_2(\cdot,y,z)(x) = \sum_{k=1}^{n}\Big\langle \frac{\log_{c(x)} y}{\|\log_{c(x)} y\|_{c(x)}}, D_x c[\xi_k]\Big\rangle_{c(x)}, \quad \xi_k \in T_x\mathcal{M}.$$

Proximal Mapping of a Second Order Difference on $\mathcal{M}$

To Compute

$$\operatorname{prox}_{\lambda d_2}(g) = \operatorname*{arg\,min}_{u\in\mathcal{M}^3}\Big\{\frac{1}{2}\sum_{i=1}^{3} d(u_i,g_i)^2 + \lambda d_2(u_1,u_2,u_3)\Big\}$$

(sub)gradient descent method requires gradient of $d_2(x,y,z) = d(c(x,z),y)$

$$\nabla_{\mathcal{M}^3} d_2 = \big(\nabla_{\mathcal{M}} d_2(\cdot,y,z), \nabla_{\mathcal{M}} d_2(x,\cdot,z), \nabla_{\mathcal{M}} d_2(x,y,\cdot)\big)^{\mathrm{T}}.$$

For $y \neq c(x,z)$ and an ONB $\{\xi_1,\ldots,\xi_n\}$ of $T_x\mathcal{M}$

- $\nabla_{\mathcal{M}} d_2(x,\cdot,z)(y) = \dfrac{\log_y c(x,z)}{\|\log_y c(x,z)\|_y} \in T_y\mathcal{M}$
- $\nabla_{\mathcal{M}} d_2(\cdot,y,z)$ by chain rule

$$\nabla_{\mathcal{M}} d_2(\cdot,y,z)(x) = \sum_{k=1}^{n}\Big\langle \frac{\log_{c(x)} y}{\|\log_{c(x)} y\|_{c(x)}}, D_x c[\xi_k]\Big\rangle_{c(x)}, \quad \xi_k \in T_x\mathcal{M}.$$

Geodesic Variation

How do small changes in x affect the geodesic?

- $\sigma_{x,\xi_k}(s)$, $k = 1, \ldots, n$, $s \in (-\varepsilon, \varepsilon)$:
  curve starting in $\sigma_{x,\xi_k}(0) = x$ with direction $\sigma'_{x,\xi_k}(0) = \xi_k$
- $\zeta_k(s)$: direction in $\sigma_{x,\xi_k}(s)$ towards z.

$\Rightarrow$ geodesic variation of the geodesic $\gamma_{\widehat{x,z}}$

$$\Gamma_k(s,t) := \exp_{\sigma_{x,\xi_k}(s)}\left(t\zeta_k(s)\right), \quad s \in (-\varepsilon, \varepsilon),\ t \in [0,T],\ T = d(x,z)$$

Jacobi Fields

Indicate directions of change along the geodesic and rephrase computation of the gradient to...

The Jacobi field J_k, $k = 1, \ldots, n$, along $\gamma_{\widehat{x,z}}$ is defined by

$$J_k(t) := \frac{\partial}{\partial s}\Gamma_k(s,t)\Big|_{s=0}, \quad t \in [0,T]$$

Lemma

$$D_x c[\xi_k] = J_k\left(\tfrac{T}{2}\right)$$

Lemma

A Jacobi field J_k fulfills the System of ODEs

$$\frac{D^2}{\mathrm{d}t^2} J_k + R(J_k, \dot\gamma_{\widehat{x,z}})\dot\gamma_{\widehat{x,z}} = 0, \qquad J_k(0) = \xi_k,\ J_k(T) = 0$$

with the Riemannian curvature tensor $R\colon T\mathcal{M} \times T\mathcal{M} \times T\mathcal{M} \to T\mathcal{M}$.

Riemannian Symmetric Spaces

...for certain manifolds there's still hope.

- For every $x \in \mathcal{M}$ exists an isometry s_x on $\mathcal{M}$, i.e.

$$s_x(x) = x, D_x s[\xi] = -\xi, \qquad \text{for all } \xi \in T_x\mathcal{M}$$

- covariant derivative

$$\nabla R = 0$$

- Examples
  - $\mathbb{S}^n$
  - Hyperbolic Spaces
  - $\mathcal{P}(s)$
  - Grasmannians

Riemannian symmetric spaces are the most beautiful and most important Riemannian manifolds.

(J.-H. Eschenburg, 1997)

A Specific Frame Along $\gamma_{\widehat{x,z}}$

Decompose the Jacobi field in Riemannian symmetric spaces

With parallel transport of an orthonormal frame $\{\Theta_1 = \Theta_1(t), \ldots, \Theta_n = \Theta_n(t)\}$, i.e.

$$J_k(t) = \sum_{i=1}^{n} a_{k,i}(t)\Theta_i(t).$$

The system of ODEs

$$\frac{D^2}{\mathrm{d}t^2}J_k + R(J_k, \dot\gamma_{\widehat{x,z}})\dot\gamma_{\widehat{x,z}} = 0, \qquad J_k(0) = \xi_k, J_k(T) = 0$$

simplifies to a a linear system of ODEs with constant coefficients

$$a''(t) + Ga(t) = 0, \qquad G := \Bigl(\bigl\langle R(\Theta_i, \dot\gamma_{\widehat{x,z}})\dot\gamma_{\widehat{x,z}}, \Theta_j\bigr\rangle_{\gamma_{\widehat{x,z}}}\Bigr)_{i,j=1}^{n}.$$

Choose $\{\xi_1, \ldots, \xi_n\}$ at $t = 0$ that diagonalize G with eigenvalues κ_i

$\Rightarrow$ Decoupled ODEs

The Derivative $D_x c[\xi_k]$ in Symmetric Spaces

Finally we are able to evaluate the Jacobi field at the mid point $T/2$

Corollary

Let κ_i denote the eigen values of G. With $T = d(x,z)$ we have for $k = 1, \ldots, n$

$$D_x c[\xi_k] = J_k\left(\tfrac{T}{2}\right) = \begin{cases} \frac{\sinh\left(\sqrt{-\kappa_k}\frac{T}{2}\right)}{\sinh(\sqrt{-\kappa_k}T)}\Theta_k\left(\frac{T}{2}\right), & \text{if } \kappa_k < 0, \\ \frac{\sin\left(\sqrt{\kappa_k}\frac{T}{2}\right)}{\sin(\sqrt{\kappa_k}T)}\Theta_k\left(\frac{T}{2}\right), & \text{if } \kappa_k > 0, \\ \frac{1}{2}\Theta_k\left(\frac{T}{2}\right), & \text{if } \kappa_k = 0. \end{cases}$$

$\Rightarrow$ Gradient descent to approximate the Proximal Mapping of the second order difference on a manifold.

Examples of Gradients $\nabla d_2(\cdot, y, z)(x)$

- the sphere $\mathbb{S}^n$
  choose $\xi_1 = \dot\gamma_{\widehat{x,z}}(0) = \log_x z$ and extend to ONB on $T_x\mathcal{M}$

$$D_x c[\xi_1] = \frac{1}{2}\,\Theta_1(\tfrac{T}{2}), \quad D_x c[\xi_k] = \frac{\sin\frac{T}{2}}{\sin T}\,\Theta_k(\tfrac{T}{2}), \quad k = 2, \ldots, n.$$

Examples of Gradients $\nabla d_2(\cdot, y, z)(x)$

- the sphere $\mathbb{S}^n$
  choose $\xi_1 = \dot\gamma_{\overset{\frown}{x,z}}(0) = \log_x z$ and extend to ONB on $T_x\mathcal{M}$

$$D_x c[\xi_1] = \frac{1}{2}\,\Theta_1(\tfrac{T}{2}),\quad D_x c[\xi_k] = \frac{\sin\frac{T}{2}}{\sin T}\,\Theta_k(\tfrac{T}{2}),\quad k = 2,\ldots,n.$$

- symmetric positive definite matrices $\mathcal{P}(s)$, $n = \frac{s(s+1)}{2}$,
  Decompose $v = \log_x z = \sum_{i=1}^{s} \lambda_i v_i v_i^{\mathrm{T}} \in T_x\mathcal{P}(s) = \{x\} \times \operatorname{Sym}(s)$ and choose

$$\xi_{ij} := \begin{cases} \frac{1}{2}(v_i v_j^{\mathrm{T}} + v_j v_i^{\mathrm{T}}), & \text{if } i = j,\\ \frac{1}{\sqrt{2}}(v_i v_j^{\mathrm{T}} + v_j v_i^{\mathrm{T}}) & \text{if } i \neq j, \end{cases},\quad 1 \leq i \leq j \leq s$$

as ONB of $T_x\mathcal{P}(s)$. From $\kappa_{i,j} = -\frac{1}{4}(\lambda_j - \lambda_j)^2$ we obtain

$$D_x c[\xi_{ij}] = \begin{cases} \frac{1}{2}\Theta_{ij}(\frac{T}{2}) & \text{if } \lambda_i = \lambda_j,\\ \frac{\sinh\left(\frac{T}{4}|\lambda_i - \lambda_j|\right)}{\sinh\left(\frac{T}{2}|\lambda_i - \lambda_j|\right)}\,\Theta_{ij}(\frac{T}{2}) & \text{if } \lambda_i \neq \lambda_j. \end{cases}$$

Minimizing the Second Order Model: An efficient Splitting

To minimize

$$\mathcal{E}(u) := \sum_{i\in\mathcal{V}} d(f_i, u_i)^2 + \alpha \sum_{i\in\mathcal{G}\setminus\{N\}} d(u_i, u_{i+1}) + \beta \sum_{i\in\mathcal{G}\setminus\{1,N\}} d_2(u_{i-1}, u_i, u_{i+1})$$

take each summand as φ_l in the CPPA: $c = 3N - 3$ proximal maps.
Improved by

- $\varphi(u_i) = d(f_i, u_i)^2$, evaluate in parallel
- $\varphi(u_i, u_{i+1}) = d(u_i, u_{i+1})$, even-odd-splitting
- $\varphi(u_{i-1}, u_i, u_{i+1}) = d_2(u_{i-1}, u_i, u_{i+1})$, splitting w. r. t. $\bmod 3$

$\Rightarrow$ reduced to $c = 6$ parallel/vector-valued proximal maps for signals
$c = 15$ for images.

Convergence of the CPPA on Manifolds

Hadamard manifold: complete Riemannian manifold $\mathcal{M}$ with

$$2d(c(x,z),c(y,z)) \leq d(x,y),\ \text{for all } x,y,z \in \mathcal{M}$$

- triangles are "thinner" than in $\mathbb{R}^n$
- smaller angle sum than in $\mathbb{R}^n$

Theorem (Exact CPPA) [Bačák, B., Steidl, Weinmann, 2015]

Let $\mathcal{M}$ be a Hadamard manifold and let $\varphi = \sum_{l=1}^{c} \varphi_l,\ \varphi_l : \mathcal{M} \to \mathbb{R}$, have a global minimizer. Assume there exist $p \in \mathcal{H}$, $C > 0$ such that for each $l = 1, \ldots, L$ and all $x, y \in \mathcal{M}$ we have

$$\varphi_l(x) - \varphi_l(y) \leq Cd(x,y)\,(1 + d(x,p))\,.$$

Then the sequence $\{x^{(k)}\}_{k\in\mathbb{N}}$ defined by the CPPA

$$x^{(k+1)} := \operatorname{prox}_{\lambda_k\varphi_c} \circ \operatorname{prox}_{\lambda_k\varphi_{c-1}} \circ \ldots \circ \operatorname{prox}_{\lambda_k\varphi_1}(x^{(k)})$$

with $\{\lambda_k\} \in \ell_2(\mathbb{Z})\backslash\ell_1(\mathbb{Z})$ converges for every $x^{(0)}$ to a minimizer of φ.

Convergence with Inexact Proximal Mappings

- our second order model functional $\mathcal{E}(u)$ fulfills these requirements of φ
- but the second order proximal maps are only approximately given

Theorem (Inexact CPPA) [Bačák, B., Steidl, Weinmann, 2015]

Let $\mathcal{M}$ be a Hadamard manifold, let φ be given as in the last Theorem. Let $\{x^{(k)}\}_{k\in\mathbb{N}}$ be the sequence generated by the inexact cyclic PPA with

$$d\Bigl(x^{(k+\frac{l}{c})}, \operatorname{prox}_{\lambda_k\varphi_l}(x^{(k+\frac{l-1}{c})})\Bigr) < \frac{\varepsilon_k}{c},$$

and

$$\sum_{k=0}^{\infty} \varepsilon_k < \infty.$$

Then the sequence $\{x^{(k)}\}_{k\in\mathbb{N}}$ converges to a minimizer of φ.

A One-Dimensional Example of Cyclic Data

Denoising a phase valued signal.

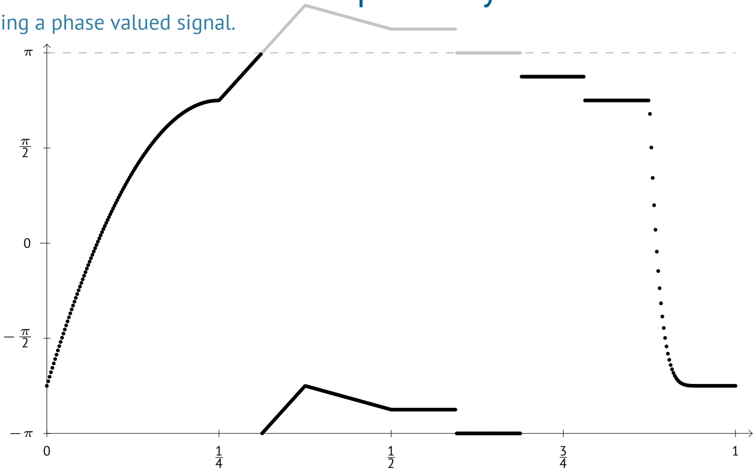

- function $f\colon [0,1] \to \mathbb{S}^1$ sampled to obtain data $f_o = (f_{o,i})_{i=1}^{500}$
- f could be a wrapped version of the gray plot, hence
- jumps $> \pi$ at $\frac{5}{16}$ and $\frac{11}{16}$ are due to the representation system

A One-Dimensional Example of Cyclic Data

Denoising a phase valued signal.

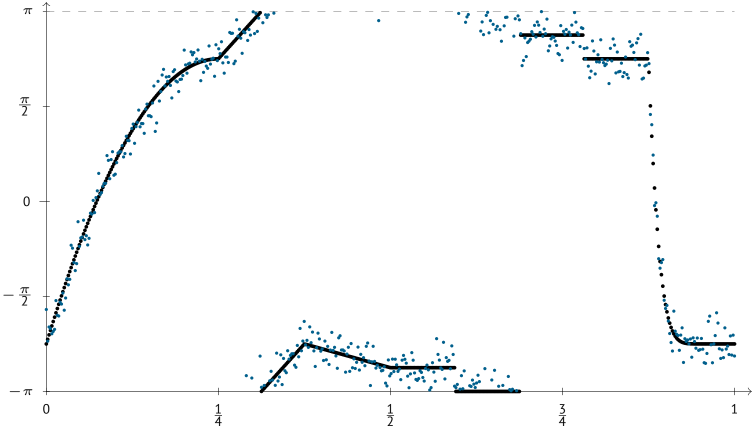

- function $f\colon [0,1] \to \mathbb{S}^1$ sampled to obtain data $f_o = (f_{o,i})_{i=1}^{500}$
- adding wrapped Gaussian noise, $\sigma = 0.2$
- noisy data $f_n = (f_0 + \eta)_{2\pi}$

A One-Dimensional Example of Cyclic Data

Denoising a phase valued signal.

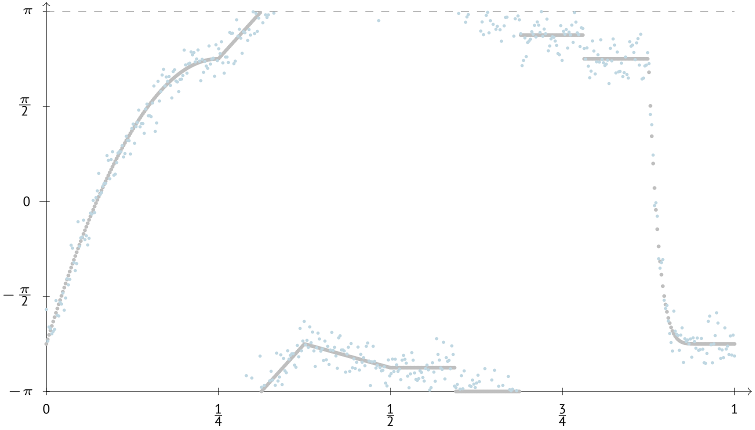

- comparison of f_o & f_n with

A One-Dimensional Example of Cyclic Data

Denoising a phase valued signal.

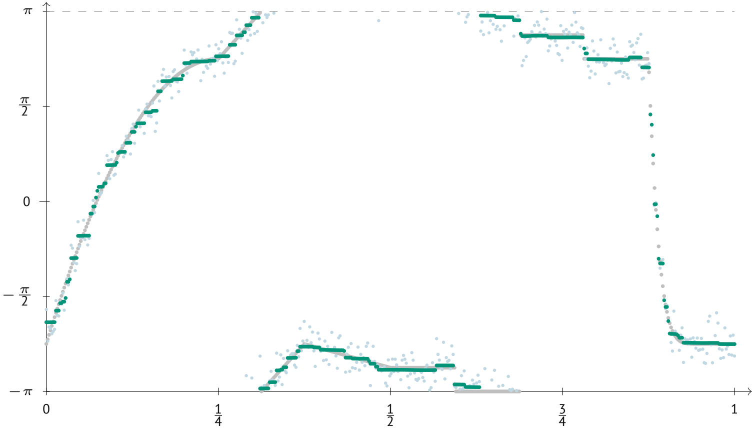

- comparison of f_o & f_n with f_1
- denoising TV_1 ($\alpha = \frac{3}{4}, \beta = 0$)
- but: stair casing

A One-Dimensional Example of Cyclic Data

Denoising a phase valued signal.

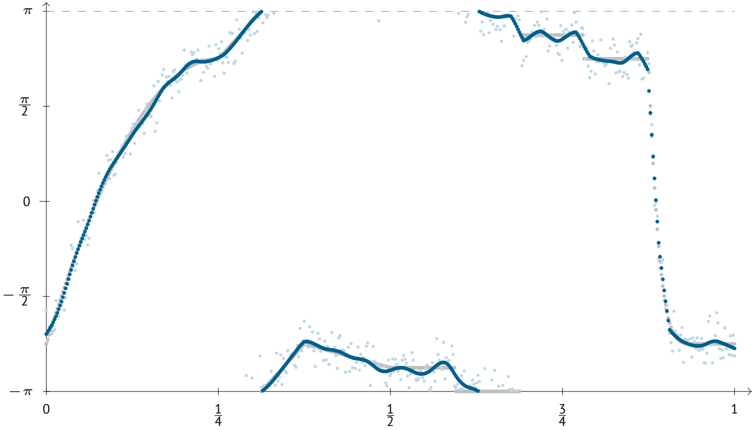

- comparison of f_o & f_n with f_2
- denoising TV_2 ($\alpha = 0$, $\beta = \frac{3}{2}$)
- but: no plateaus

A One-Dimensional Example of Cyclic Data

Denoising a phase valued signal.

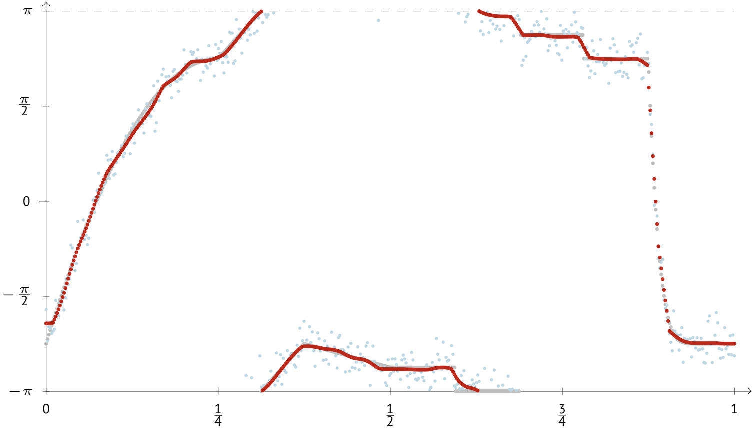

- comparison of f_o & f_n with f_3
- denoising TV_1 & TV_2 ($\alpha = \frac{1}{2}, \beta = 1$)
- smallest mean squared error

Combined Inpainting and Denoising

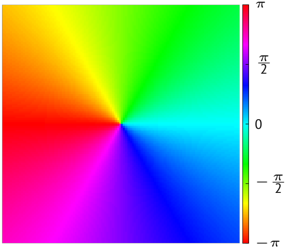

original image

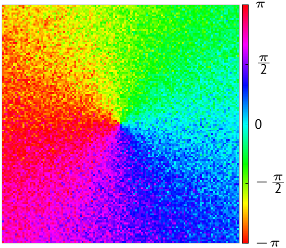

noisy image, $\sigma = 0.3$

Combined Inpainting and Denoising

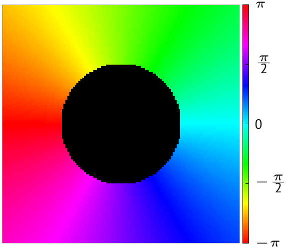

original image (lost area in black)

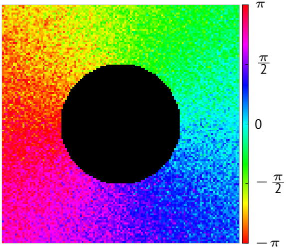

noisy image, $\sigma = 0.3$

Combined Inpainting and Denoising

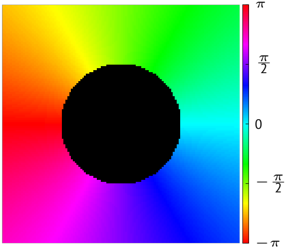

original image (lost area in black)

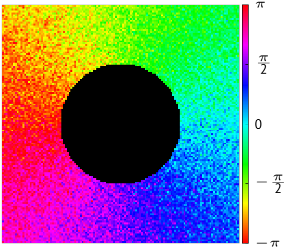

noisy image, $\sigma = 0.3$

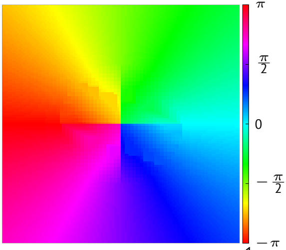

noiseless model, $\alpha = \frac{1}{8}$.

Combined Inpainting and Denoising

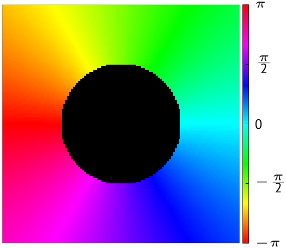

original image (lost area in black)

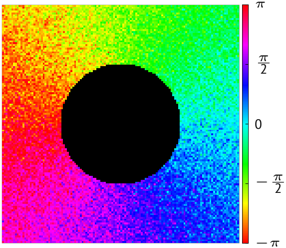

noisy image, $\sigma = 0.3$

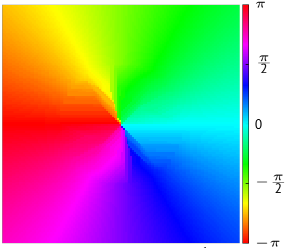

noiseless model, $\alpha = \frac{1}{8}$ (& diags).

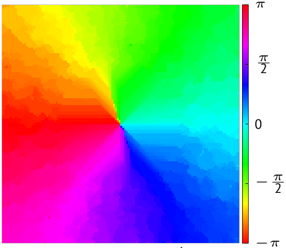

noisy model, $\alpha = \frac{1}{8}$ (& diags).

Combined Inpainting and Denoising

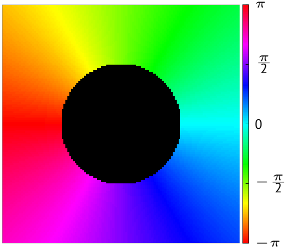

original image (lost area in black)

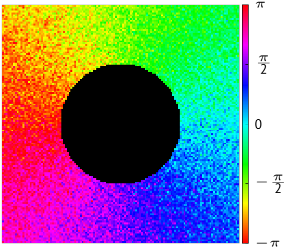

noisy image, $\sigma = 0.3$

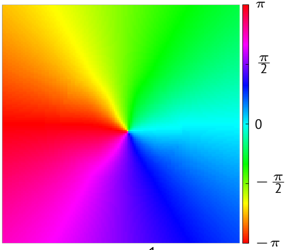

noiseless model, $\alpha = \frac{1}{8}$ (& diags), $\beta = \gamma = \frac{1}{4}$.

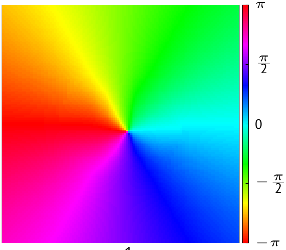

noisy model, $\alpha = \frac{1}{8}$ (& diags), $\beta = \gamma = \frac{1}{4}$.

Bernoulli's Lemniscate on the Sphere $\mathbb{S}^2$

$$\gamma(t) := \frac{a\sqrt{2}}{\sin^2(t)+1}\bigl(\cos(t), \cos 1 \sin(t)\bigr)^{\mathrm{T}}, \quad t \in [0, 2\pi], a = \frac{\pi}{2\sqrt{2}}.$$

Generate a sphere-valued signal by putting it into the tangential plane of the north pole

$$\gamma_S(t) = \log_p(\gamma(t)), p = (0,0,1)^{\mathrm{T}}$$

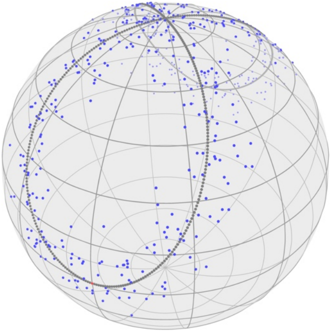

noisy lemniscate of Bernoulli on $\mathbb{S}^2$, Gaussian noise, $\sigma = \frac{\pi}{30}$, on $T_p\mathbb{S}^2$.

Bernoulli's Lemniscate on the Sphere $\mathbb{S}^2$

$$\gamma(t) := \frac{a\sqrt{2}}{\sin^2(t)+1}\bigl(\cos(t), \cos 1 \sin(t)\bigr)^{\mathrm{T}}, \quad t \in [0, 2\pi], a = \frac{\pi}{2\sqrt{2}}.$$

Generate a sphere-valued signal by putting it into the tangential plane of the north pole

$$\gamma_S(t) = \log_p(\gamma(t)), p = (0,0,1)^{\mathrm{T}}$$

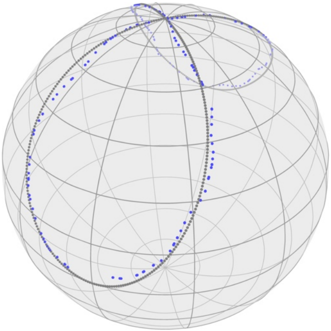

reconstruction with TV_1, $\alpha = 0.21$, $\mathrm{MAE} = 4.08 \times 10^{-2}$.

Bernoulli's Lemniscate on the Sphere $\mathbb{S}^2$

$$\gamma(t) := \frac{a\sqrt{2}}{\sin^2(t)+1}\bigl(\cos(t), \cos 1 \sin(t)\bigr)^{\mathrm{T}}, \quad t \in [0, 2\pi], a = \frac{\pi}{2\sqrt{2}}.$$

Generate a sphere-valued signal by putting it into the tangential plane of the north pole

$$\gamma_S(t) = \log_p(\gamma(t)), p = (0,0,1)^{\mathrm{T}}$$

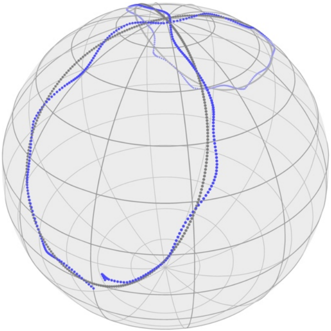

reconstruction with TV_2, $\alpha = 0$, $\beta = 10$, $\mathrm{MAE} = 3.66 \times 10^{-2}$.

Bernoulli's Lemniscate on the Sphere $\mathbb{S}^2$

$$\gamma(t) := \frac{a\sqrt{2}}{\sin^2(t)+1}\big(\cos(t), \cos 1 \sin(t)\big)^{\mathrm{T}}, \quad t \in [0, 2\pi], a = \frac{\pi}{2\sqrt{2}}.$$

Generate a sphere-valued signal by putting it into the tangential plane of the north pole

$$\gamma_S(t) = \log_p(\gamma(t)), p = (0,0,1)^{\mathrm{T}}$$

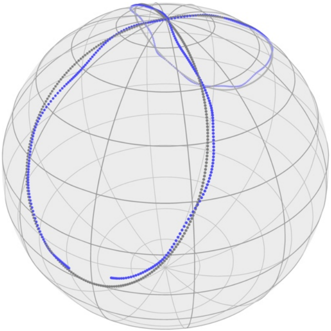

reconstruction with TV_1 & TV_2, $\alpha = 0.16$, $\beta = 12.4$, $\mathrm{MAE} = 3.27 \times 10^{-2}$.

$\mathbb{S}^2$-valued data: An Image of Directions

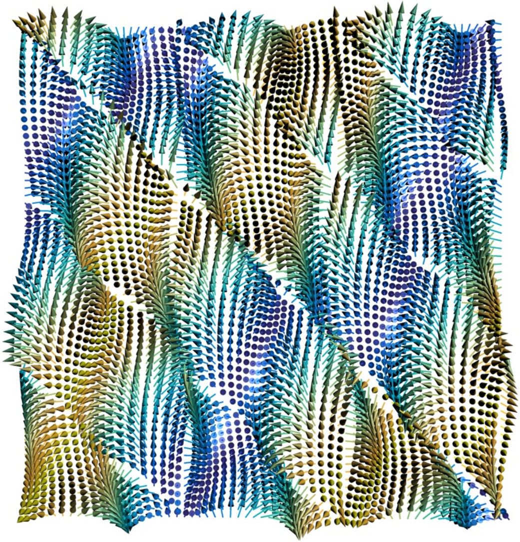

original data

$\mathbb{S}^2$-valued data: An Image of Directions

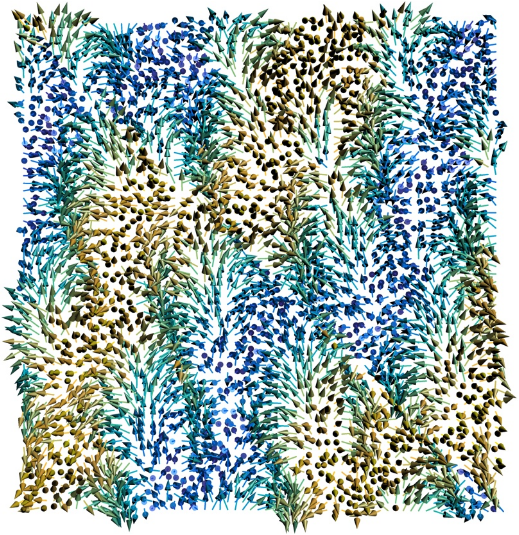

noisy data

$\mathbb{S}^2$-valued data: An Image of Directions

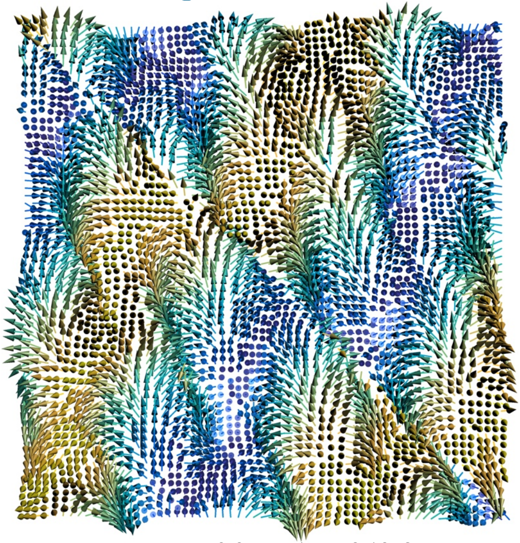

TV_1 model, $\alpha = 0.035$, MAE $= 0.1879$.

$\mathbb{S}^2$-valued data: An Image of Directions

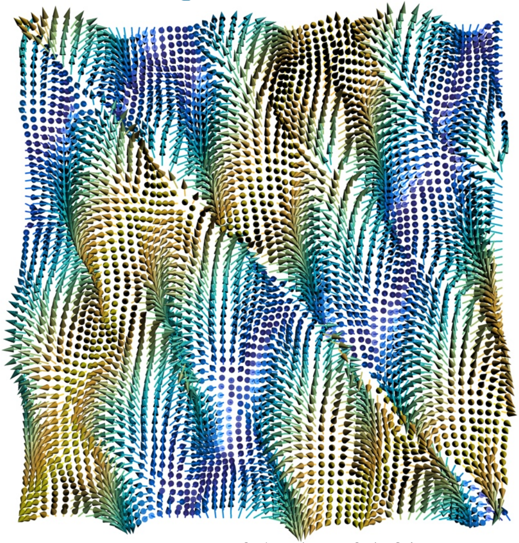

TV_2 model, $\beta = 8.6$, MAE $= 0.1394$

Inpainting of $\mathcal{P}(3)$ valued images

Illustrate symmetric positive definite 3×3 matrices as ellipsoids

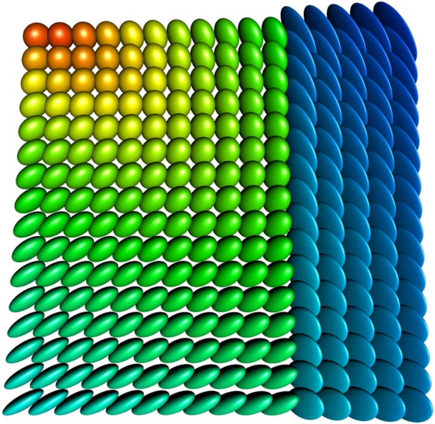

original data

Inpainting of $\mathcal{P}(3)$ valued images

Illustrate symmetric positive definite 3×3 matrices as ellipsoids

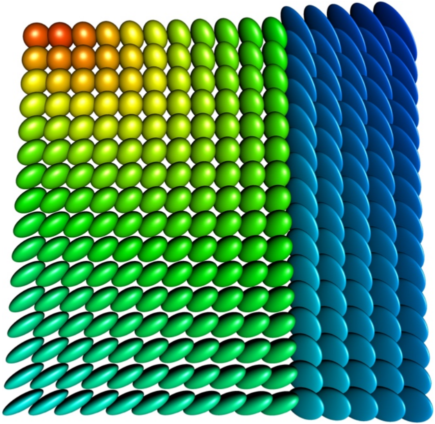

original data

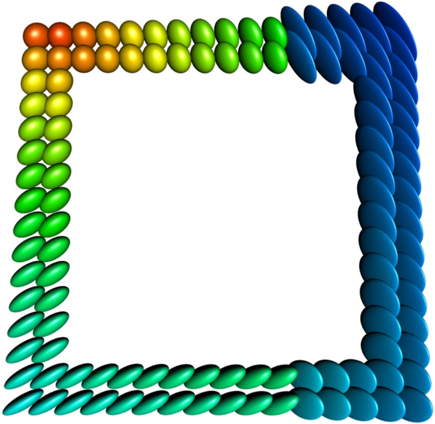

lost (a lot of) data

Inpainting of $\mathcal{P}(3)$ valued images

Illustrate symmetric positive definite 3×3 matrices as ellipsoids

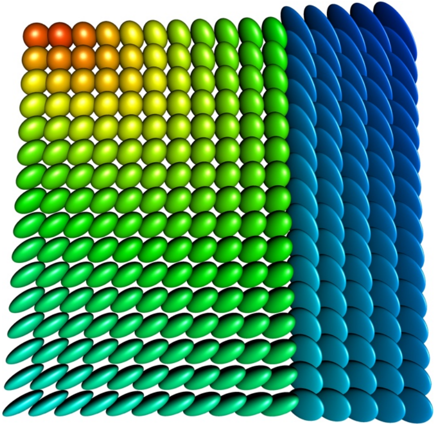

original data

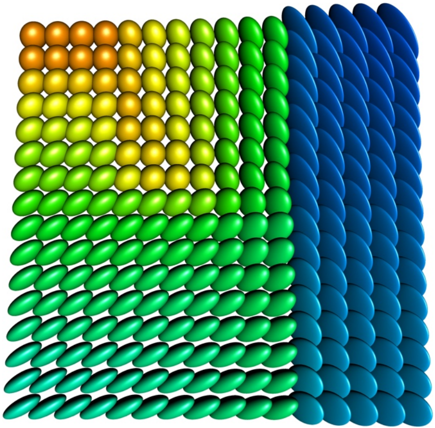

inpainted with $\alpha = \beta = 0.05$, MAE $= 0.0929$

Inpainting of $\mathcal{P}(3)$ valued images

Illustrate symmetric positive definite 3×3 matrices as ellipsoids

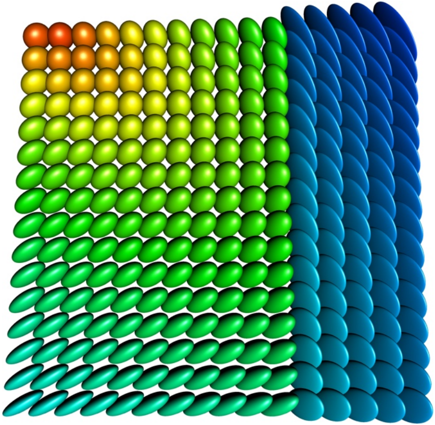

original data

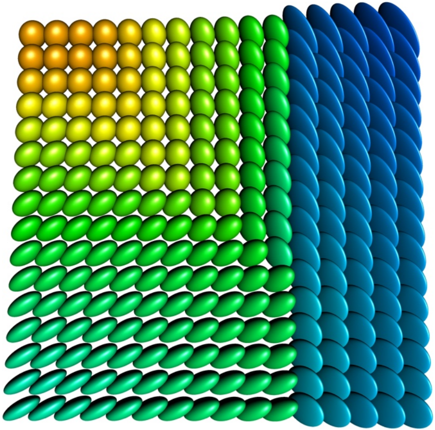

inpainted with $\alpha = 0.1$, MAE $= 0.0712$

Diffusion Tensor Magnetic Resonance Imaging

Dataset $\mathcal{P}(3)^{112\times112\times50}$ of the human head, traversal plane $z = 28$

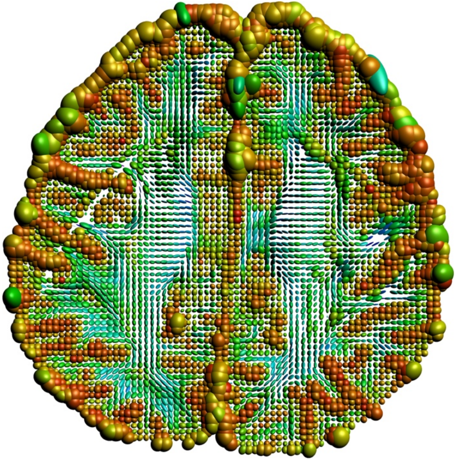

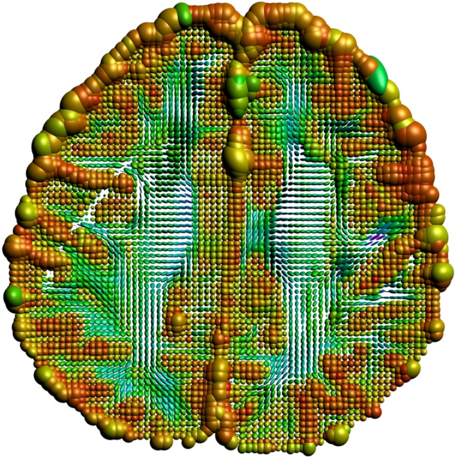

original data, denoised, $\alpha = 0.01$, $\beta = 0.05$

(Data available from The Camino Project, cmic.cs.ucl.ac.uk/camino)

Diffusion Tensor Magnetic Resonance Imaging

Dataset $\mathcal{P}(3)^{112\times112\times50}$ of the human head, traversal plane $z = 28$

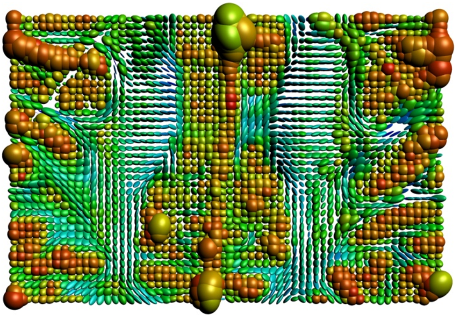

original data,

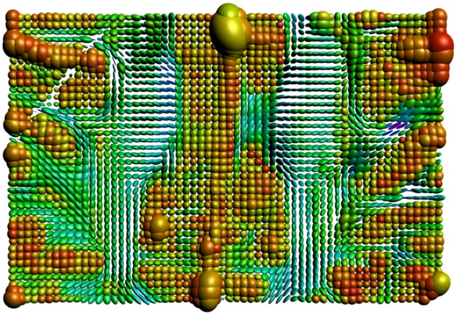

denoised, $\alpha = 0.01$, $\beta = 0.05$

(Data available from The Camino Project, cmic.cs.ucl.ac.uk/camino)

a detail

Conclusion

We have for manifold valued images $f\colon \mathcal{V} \to \mathcal{M}$

- a model for second order differences
- a first and second order TV-type functional $\mathcal{E}(u)$
- applicable to denoising and inpainting
- cyclic proximal point algorithm to minimize the functional $\mathcal{E}(u)$
- computed the proximal mappings using Jacobi fields
- proof of convergence

Future work

- an isotropic second order TV
- other couplings
- other algorithms, e.g. a stochastic Douglas-Rachford algorithm

Literature

[1] M. Bačák, R. Bergmann, G. Steidl, and A. Weinmann. A second order non-smooth variational model for restoring manifold-valued images. *Preprint, ArXiv #1506.02409*, 2015.

[2] R. Bergmann, R. H. Chan, R. Hielscher, J. Persch, and G. Steidl. Restoration of Manifold-Valued Images by Half-Quadratic Minimization. *Preprint, ArXiv #1505.07029*, 2015.

[3] R. Bergmann, F. Laus, G. Steidl, and A. Weinmann. Second order differences of cyclic data and applications in variational denoising. *SIAM J. Imaging Sci.*, 2014.

[4] R. Bergmann and A. Weinmann. A second order TV-type approach for inpainting and denoising higher dimensional combined cyclic and vector space data. *Preprint, ArXiv #1501.02684*, 2015.

[5] R. Bergmann and A. Weinmann. Inpainting of cyclic data using first and second order differences. *EMMCVPR 2015*, 2015.

Literature

[1] M. Bačák, R. Bergmann, G. Steidl, and A. Weinmann. A second order non-smooth variational model for restoring manifold-valued images. *Preprint, ArXiv #1506.02409*, 2015.

[2] R. Bergmann, R. H. Chan, R. Hielscher, J. Persch, and G. Steidl. Restoration of Manifold-Valued Images by Half-Quadratic Minimization. *Preprint, ArXiv #1505.07029*, 2015.

[3] R. Bergmann, F. Laus, G. Steidl, and A. Weinmann. Second order differences of cyclic data and applications in variational denoising. *SIAM J. Imaging Sci.*, 2014.

[4] R. Bergmann and A. Weinmann. A second order TV-type approach for inpainting and denoising higher dimensional combined cyclic and vector space data. *Preprint, ArXiv #1501.02684*, 2015.

[5] R. Bergmann and A. Weinmann. Inpainting of cyclic data using first and second order differences. *EMMCVPR 2015*, 2015.

Thank you for your attention.